MD simulation for H$_2$ formation on amorphous ice

Junko Takahashi[1,2,3*]

[1]*National Astronomical Observatory, 2-21-1, Osawa, Mitaka, Tokyo 181-8588, Japan*
[2]*Institute for Fundamental Chemistry, 34-4, Takano-Nishihiraki-cho, Sakyo-ku, Kyoto 606-8103, Japan*
[3]*Department of Physics and Astronomy, University College London, Gower Street, London WC1E 6BT, U.K.*

Recent advances in a series of studies based on the molecular dynamics (MD) computer simulation that was performed to investigate the whole of H$_2$ formation process on the surface of dust grains throughout within a single model are reviewed. Amorphous water ice slabs were generated at 10 K and 70 K as a model surface of dust grains, and then the first and second incident H atoms were thrown onto the surface. The following fundamental processes of H$_2$ formation via two H atoms' recombination, H + H $\rightarrow$ H$_2$, were studied in detail; 1) the sticking of H atom onto the surface, 2) the diffusion of H atom on the surface, 3) the reaction of two H atoms on the surface, 4) the ejection of H$_2$ from the ice surface. The sticking probability, the mobility, the reaction probability, and the ejection lifetime were selfconsistantly obtained for the above processes. The product energy distribution of H$_2$ molecules formed on icy mantles of dust grains was also studied, and it was found that H$_2$ molecules can be highly vibrationally excited by formation pumping mechanism.

1. Introduction

It is widely accepted that formation of interstellar molecular hydrogens ought to occur predominantly on the surface of dust grains. The dust grains generally have icy mantles with amorphous structure, predominantly of H$_2$O, which accumulate on solid particles inside dark clouds (see, e.g., Williams, 1993; Herbst, 1995).

The fundamental processes of H$_2$ formation via two H atoms' recombination, H + H $\rightarrow$ H$_2$, on the surface of dust grains are considered as follows; 1) sticking of incident H atoms onto the dust surface, 2) diffusion of H atoms over the surface, 3) reaction of two H atoms on the surface, and 4) ejection of product H$_2$ molecule from the surface back into the gas phase (see, e.g., Williams, 1993; Herbst, 1995). In order to know chemical evolution in various interstellar regions, it is very important to determine the rate constant for H$_2$ formation on dust grains. For this purpose, the formation mechanism of H$_2$ on the grain surface should be investigated from an overall point of view, and the sticking probability, diffusion constant, reaction probability, and ejection rate should be obtained.

It has been considered that there are two sources of excitation contributing to the rovibrational emission spectrum of interstellar H$_2$, UV pumping and collisional excitation. However, recent astronomical observations have required the third excitation source by formation pumping (see, e.g., Usuda, 1996). In order to determine the effect of the formation pumping, it is also very important to study the energy distribution in the H$_2$ formation process on the surface of dust grains (see, e.g., Duley, 1986, 1993).

Several authors have previously studied on one of fundamental processes of H$_2$ formation on dust grains or the product energy distribution of H$_2$ (Hollenbach and Salpeter, 1970; Hunter and Watson, 1978; Leitch-Devlin and Williams, 1985; Duley and Williams, 1986, 1993; Buch, 1990; Zhang and Buch, 1990; Buch and Zhang, 1991; Buch and Devlin, 1993, 1994). However, there have been no studies according to the policy that the sticking probability, diffusion constant, reaction probability, ejection rate, and product energy distribution should be obtained selfconsistantly within a single model. Therefore, recent studies by Masuda and Takahashi (1997), Masuda *et al.* (1998), and Takahashi *et al.* (1999a,b) have been performed to carry out this policy by using molecular dynamics (MD) computer simulation. This review focuses on collecting these studies into an article showing advances in this method.

In this model, the slab-shaped amorphous water ice was produced by MD simulation, as a realistic model surface of icy mantles of dust grains. Then, two H atoms were successively thrown onto the surface, and their dynamical behaviers were investigated by MD simulation. All of the fundamental processes of H$_2$ formation on the surface of dust grains, sticking, diffusion, reaction, and ejection, were studied in detail. The product energy distribution of H$_2$ formed on the ice surface was also studied. In Section 2, the methods of MD simulation, computational details, and energy analysis are described. The results and discussions about amorphous water ice, sticking process, diffusion process, reaction process, ejection process, and product energy distribution are presented in Section 3. The conclusions are summarized in Section 4.

---

*Present address: National Astronomical Observatory.

2. Methods
2.1 MD simulation

Classical MD simulation is a well established technique for studying molecular processes in the field of physical chemistry. In this technique, positions, velocities, and forces of the molecules are obtained as functions of time by solving numerical Newtonian equations of motion for the many-body system. The total potential of the system is generally given as a sum of pair potentials.

Despite the limitation of the classical treatment of motions, it has provided us with much realistic information about the molecular processes when they are dominated by the thermal dynamics (see, e.g., Hansen and McDonald, 1986). Our model, where the hydrogen atom or molecule is physisorbed on the surface of icy mantles and have excess thermal energy during most of the processes, could be well treated by this technique (Masuda and Takahashi, 1997; Masuda et al., 1998). The quantum treatment should be especially employed for the diffusion process of the H atom after it loses the excess thermal energy and becomes trapped on the surface of dust grains (Takahashi et al., 1998).

2.2 Computational details

For the first stage of our MD simulation, the slab-shaped amorphous water ice was generated under periodic boundary conditions. As the initial conditions, 1000 water molecules were placed randomly in the unit cell, and an equilibrium structure of amorphous water ice slab was obtained after 10 ps (picoseconds) (1 ps $= 10^{-12}$ s) run, where the time step was taken to be 1 fs (femtosecond) (1 fs $= 10^{-15}$ s). The volume of the slab in the unit cell was about 40 Å $\times$ 40 Å $\times$ 20 Å. For the second stage, we performed MD simulation for the system consisting of both the amorphous water ice slab and the first incident H atom thrown onto the surface. For the third stage, the second incident H atom was thrown onto the above system. The time steps and time durations for the second and third stages were taken to be 0.1 fs and 5 ps, respectively. The temperatures of the amorphous water ice slabs were kept at 10 K and 70 K. Initial kinetic temperatures of incident H atoms were set at 10 K and 70 K, respectively, for 10 K and 70 K ice slabs. In these simulations, the full dynamics was treated for all of the atoms and molecules in the system, and thus the energy transfer from H atoms and H$_2$ to the amorphous water ice was taken into account directly.

The potential model used for a pair of H$_2$O molecules was TIPS2 (Transferable Intermolecular Potential of the second version) by Jorgensen (1982):

$$V_{H_2O-H_2O} = \frac{A}{r_{OO}^{12}} - \frac{C}{r_{OO}^{6}} + \sum_i \sum_j \frac{q_i q_j e^2}{r_{ij}}. \quad (1)$$

In this equation, the first and second terms are the Lennard-Jones parts and the third is the Coulomb part, where two positive charges are located on H atoms (q_H) and one negative charge is at a distance of 0.15 Å from the oxygen atom on the bisector of the H–O–H angle (q_M); i and j indicate the positions of three charges of H$_2$O and H$_2$O', respectively; r_{OO} is the distance between the two oxygen atoms; r_{ij} is the distance between the positions i and j; e is the unit electric charge; A, C, q_H, and q_M are empirical parameters (see Table 1). This potential function was modelled for the rigid water molecules.

Table 1. Parameters in Eqs. (1)–(4) (after Herzberg 1950; Jorgensen 1982; Zhang et al. 1991).

A	695,000 kcal Å^{12}/mol
C	600 kcal Å^6/mol
q_H	0.535
q_M	-1.070
$\varepsilon_{0,0}$	0.44106 kcal/mol
$\varepsilon_{1,0}$	-0.03884 kcal/mol
$\varepsilon_{2,0}$	0.03515 kcal/mol
$\varepsilon_{2,2}$	0.14549 kcal/mol
$\sigma_{0,0}$	3.00 Å
$\sigma_{1,0}$	3.30 Å
$\sigma_{2,0}$	2.98 Å
$\sigma_{2,2}$	2.92 Å
r_e	0.74166 Å
D_e	109.5 kcal/mol
ω_e	4395.24 cm^{-1}

For the pair potential between an H atom and an H$_2$O molecule, the potential model by Zhang et al. (1991) was employed:

$$V_{H-H_2O} = \sum_{l,m} 4\varepsilon_{l,m} \left[\left(\frac{\sigma_{l,m}}{r} \right)^{12} - \left(\frac{\sigma_{l,m}}{r} \right)^{6} \right] Y_{l,m}(\theta, \phi). \quad (2)$$

This potential function is made of the Lennard-Jones part and the spherical harmonics $Y_{l,m}(\theta, \phi)$. The origin is placed on the oxygen atom of H$_2$O, r is the distance between the incident H atom and the oxygen atom, and θ and ϕ are the spherical angles. The potential parameters, $\varepsilon_{l,m}$ and $\sigma_{l,m}$, were prepared using the results of ab initio molecular orbital calculations (see Table 1).

The Morse-type potential function with experimental parameters for an H$_2$ molecule (Herzberg, 1950) was used as the interaction potential between the two H atoms:

$$V_{H-H} = D_e \left[1 - \exp\{-\beta(r - r_e)\} \right]^2 - D_e \quad (3)$$

$$\beta = \left(\frac{\mu c^2}{2D_e} \right)^{\frac{1}{2}} \omega_e \quad (4)$$

where r is the distance between the two H atoms; μ is the reduced mass of an H$_2$ molecule; r_e is its equilibrium value; D_e is the dissociation energy; ω_e is the harmonic frequency (see Table 1).

In the present MD simulation, H$_2$O molecules were treated as rigid and the SHAKE-Verlet algorithm was used for numerical integration with the quaternion's formalism. This model includes only intermolecular modes (translational vibrations) of H$_2$O, while librational (hindered rotational) and intramolecular vibrational modes of H$_2$O are neglected. This approximation might reduce the interaction between the product H$_2$ molecule and the neibouring H$_2$O molecules. However, it is known that intramolecular vibrational frequencies (1650–3380 cm^{-1} in the pure H$_2$O ice) and librational frequencies (about 500–1000 cm^{-1}) are so high that their contribution to the heat capacity can be negligible below 80 K (Fletcher, 1970; Flubacher et al., 1960). Therefore, it

is a good approximation to consider intermolecular frequencies (below about 500 cm^{-1}) for the energy transmission in the H_2O ice at 10 K and 70 K.

The temperatures of the amorphous water ice slab were kept at 10 K and 70 K by rescaling velocities of H_2O molecules at every time step. This procedure was done to mimic the canonical ensemble at a given thermodynamical temperature for H_2O molecules. When the temperature rescaling was switched off, the background temperatures of the amorphous water ice were still kept at 10 K and 70 K within a temperature fluctuation of 1%. Thus, it was found that there is little error in numerical integrations for the present system.

2.3 Product energy analysis

The energy analysis of an H_2 molecule formed on the amorphous water ice surface was performed. The total kinetic energy (T_{total}) was numerically separated into the vibrational kinetic energy (T_{vib}), the rotational kinetic energy (T_{rot}), and the translational kinetic energy (T_{trans}) at each time step.

The total energy E_{total} of the product H_2 was defined as the time average of the sum of T_{total} and potential energies including the Morse-type H–H potential energy (V_{H-H}) and the interaction energy between H_2 and amorphous water ice after H_2 was ejected from the ice surface. The vibrational energy E_{vib} was defined as the time average of the sum of T_{vib} and V_{H-H} after H_2 was ejected. The translational energy E_{trans} was defined as the time average of T_{trans} after H_2 was ejected. The rotational energy E_{rot} was defined by $E_{total} - E_{trans} - E_{vib}$.

Although the energies obtained in this simulation are classical, it is possible to make them correspond approximately to the quantum vibrational energy levels ($v = 0$–14). In the present work, we regarded classical energy between the energy levels v and $v + 1$ as being at the level v (see Table 2). The evaluated maximum error in this approximation is considered to be the extent of energy between one vibrational energy level and the adjacent one.

3. Results and Discussion
3.1 Amorphous water ice

It is considered that the amorphous water ice has a high-density structure (about 1.1 g/cm^3) below 38 K and a low-density structure (about 0.94 g/cm^3) above 68 K (Jenniskens and Blake, 1994; Jenniskens *et al.*, 1995). The amorphous water ice slabs generated at 10 K and 70 K by our MD simulation are shown in Fig. 1 (after Masuda *et al.*, 1998). Their densities were found to be about 1.07 g/cm^3 and about 0.93 g/cm^3, respectively. As was discussed previously, the O–O distance radial distribution functions at 10 K and 70 K were also found to be in good agreement with those of high-density and low-density amorphous water ice produced experimentally. Thus, we consider that the present amorphous water ice slabs are good models for the surface of icy mantles of dust grains (Masuda and Takahashi, 1997; Masuda *et al.*, 1998).

3.2 Sticking process of a hydrogen atom

The sticking process of the H atom onto the icy surface of dust grains was studied by the second stage of our MD simulation (Masuda *et al.*, 1998). The behaviours of the H atom thrown onto the amorphous water ice are classified into the sticking case and the scattered one, as are shown in Fig. 2 (after Masuda *et al.*, 1998). In the scattered case, the incident H atom went back to the initial height within 5 ps after hopping several times on the ice surface. On the other hand, in the sticking case, it was found that it took about 3 ps until the temperature of adsorbed H atoms became in equilibrium with the slab temperature. Therefore, we considered that 5 ps of the simulation period was adequate.

The sticking probabilities for incident H atoms with ini-

Table 2. Quantum vibrational energy levels of H_2 and classical vibrational energies corresponding to them.

Quantum number v	(quantum) E_v [kcal/mol]	(classical) E_{vib} [kcal/mol]
0	6.3	0.0–18.1
1	18.2	18.2–29.3
2	29.4	29.4–39.9
3	40.0	40.0–49.8
4	49.9	49.9–59.1
5	59.2	59.2–67.7
6	67.8	67.8–75.6
7	75.7	75.7–82.9
8	83.0	83.0–89.5
9	89.6	89.6–95.3
10	95.4	95.4–100.2
11	100.3	100.3–104.3
12	104.4	104.4–107.3
13	107.4	107.4–109.0
14	109.1	109.1–109.5

10 K   1.07 g/cm^3 high-density amorphous water ice

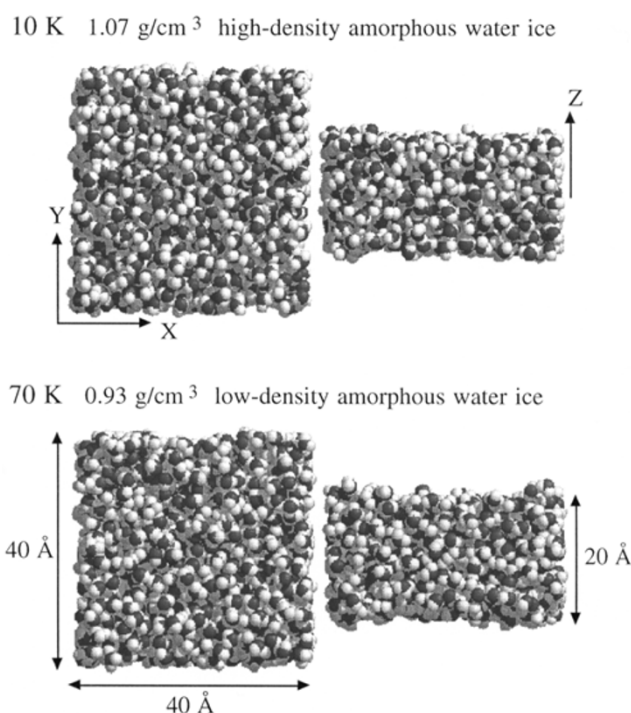70 K   0.93 g/cm^3 low-density amorphous water ice

Fig. 1. The 1st stage of MD simulation—amorphous water ice slabs generated at 10 K and 70 K (after Masuda *et al.*, 1998).
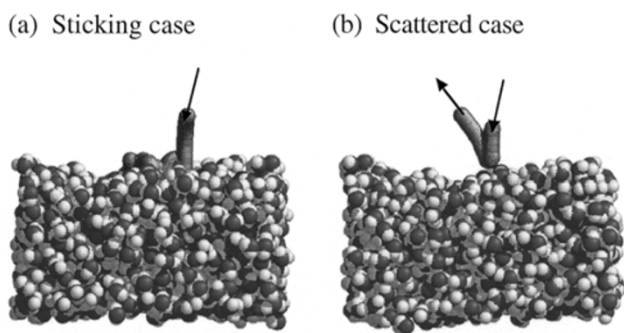
Fig. 2. The 2nd stage of MD simulation—two cases in the sticking process of an incident H atom onto the amorphous water ice (after Masuda *et al.*, 1998).

Table 3. Sticking probability of an incident H atom on the amorphous water ice (after Masuda *et al.*, 1998).

| Temperature | | Number of simulations | | | Sticking |
Ice	H atom	Sticking	Scattered	Total	probability
10 K	10 K	59	0	59	1.00
10 K	100 K	61	1	62	0.98
10 K	350 K	30	27	57	0.53
70 K	70 K	61	1	62	0.98
70 K	100 K	55	9	64	0.86
70 K	350 K	34	31	65	0.52

tial kinetic temperatures of 10–350 K were examined. The results are shown in Table 3 (after Masuda *et al.*, 1998). There is seen a clear tendency that the sticking probability becomes smaller as the kinetic temperature of the incident H atom becomes higher. Since the present amorphous water ice is a slab-shaped one with infinite area, the value of sticking probability for it is considered to be larger than that for small ice clusters (Masuda *et al.*, 1998).

3.3 Diffusion process of a hydrogen atom

The diffusion process of the H atom on the icy surface of dust grains was studied also by the second stage of our MD simulation (Masuda *et al.*, 1998). In the sticking cases, the incident H atoms initially diffused on the surface of amorphous water ice via thermal hopping mechanism for 1–3 ps and then became trapped in one of the stable sites. The average total energy of an impinging H atom gradually decreased, because a part of energy was absorbed by amorphous water ice during an H atom's hopping process. When the average total energy of the incident H atom became smaller than the potential energy barrier of a site, it was trapped there. Once an incident H atom was trapped, none was found to restart diffusing within the time duration in our MD simulation (5–10 ps).

The mobilities in the diffusion process of the H atom are classified into the one *before* trapped and that *after* trapped. The average migration length and time of the impinging H atom during the surface hopping process were calculated as the measure of the mobility *before* trapped, which were found to depend just on the temperature of the icy surface of dust grains. On the other hand, the time-scale for the H atom's movement from the trapping site to a neighboring site via thermal hopping mechanism was estimated as the measure of the mobility *after* trapped. The results are shown in Table 4 (after Masuda *et al.*, 1998).

Naturally, under such low temperatures as 10 K and 70 K, the quantum mechanical tunneling effect might be large in the diffusion process of the H atom. In order to estimate this effect, a new formalism by using the differential diffusion constant was recently developed (Takahashi *et al.*, 1998). In future work, the diffusion constant including both thermal hopping and quantum tunneling mechanisms will be calculated.

3.4 Reaction process of two hydrogen atoms

The reaction process of two hydrogen atoms on the icy surface of dust grains was studied by the third stage of our MD simulation (Takahashi *et al.*, 1999a). Two reaction cases were observed in which H$_2$ molecules are produced on the dust surface (see, e.g., Williams, 1993; Herbst, 1995). The first is the Langmuir-Hinshelwood case, in which the second incident H atom sticks on the grain surface and then diffuses into the vicinity of the site where the first H atom is trapped (Case (a), see Fig. 3(a)). The second is the Eley-Rideal case, in which the second H atom in the gas phase strikes directly the first H atom adsorbed on the dust surface (Case (b), see Fig. 3(b)). The third reaction case was also observed in our MD simulation, where two H atoms met and reacted but were almost elastically scattered each other without H$_2$ being stabilized (Case (c), see Fig. 3(c)).

There were many other MD trajectories where two H atoms could not react during the limited simulation time. It was found that they recombined when they approached each other within about 3.5 Å, while they could not encounter each other and diffused away if the minimum distance between them was more than the critical distance. Thus, the effective reactive cross-section was evaluated at about 40 Å^2.

The excess energy released when H$_2$ molecule is formed via two H atoms' recombination is about 109.5 kcal/mol, which is very large, compared with the interaction energy between two H$_2$O molecules being 6 kcal/mol and that between H and H$_2$O being 0.3 kcal/mol. In our MD simulation, the excess energy by H$_2$ formation can be absorbed by the amorphous water ice through the coupling of the H$_2$–H$_2$O libration with the intermolecular vibrational modes of H$_2$O molecules in the ice. When a part of excess energy was effectively absorbed by the amorphous water ice during the two H atoms' reacting process, H$_2$ could be formed (Cases (a) and (b)). When not, almost elastic collision of two H atoms occured (Case (c)).

Because of limitation of run time in the present MD simulation, the second H atom was intentionally thrown into the vicinity of the first H atom. Therefore, case (b) occured more frequently, and there is little significance in the ratios of cases (a) and (b). The reaction probability of the incident two H atoms on the amorphous water ice is defined as the sum of probabilities of cases (a) and (b). The present definition of the reaction probability is not a global one, but a microscopic one. The results are shown in Table 5 (after Takahashi *et al.*, 1999a) and they are found to be almost unity.

3.5 Ejection process of a molecular hydrogen

The ejection process of a molecular hydrogen from the icy surface of dust grains was studied also by the third stage of
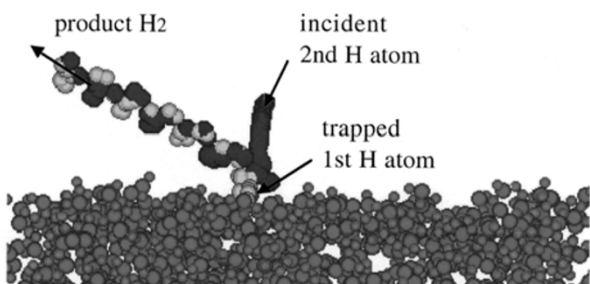
Table 4. Mobility of an incident H atom on the amorphous water ice (after Masuda *et al.*, 1998).

Temperature		Mobility *before* trapped		Mobility *after* trapped
Ice	H atom	Migration length	Migration time	Time-scale for removing
10 K	10 K	60 Å	1682 fs	10^{34} years
70 K	70 K	140 Å	2688 fs	10^{-5} seconds

(a) Langmuir-Hinshelwood case
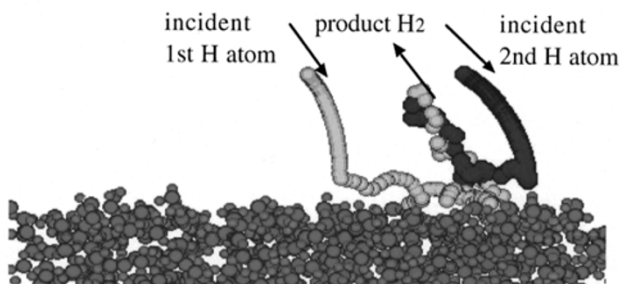
(b) Eley-Rideal case

(c) Elastic scattering case
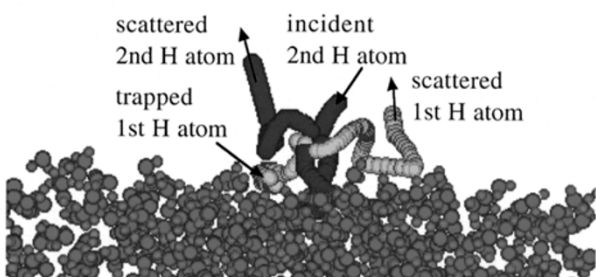
Fig. 3. The 3rd stage of MD simulation—three cases in the reaction process of two H atoms on the amorphous water ice (after Takahashi *et al.*, 1999a).

Table 5. Reaction probability of two H atoms on the amorphous water ice (after Takahashi *et al.*, 1999a).

Temperature		Number of simulations				Reaction
Ice	H atom	(a)	(b)	(c)	Total	probability
10 K	10 K	31	58	5	94	0.95
70 K	70 K	34	56	6	96	0.94

Table 6. Time-scale for the product H₂ ejected from the amorphous water ice (after Takahashi *et al.*, 1999a).

Temperature		Lifetimes of ejection		
Ice	H atom	(a)	(b)	Average
10 K	10 K	299 fs	650 fs	528 fs
70 K	70 K	445 fs	507 fs	483 fs
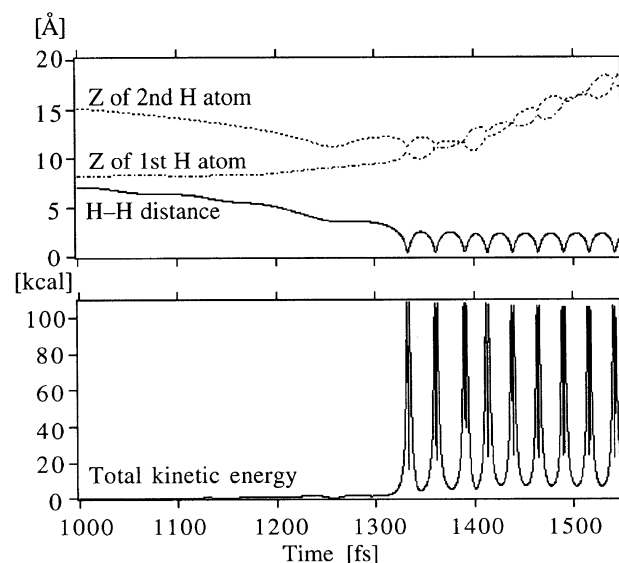
Fig. 4. Time dependences of the H–H distance, the height Z of each H atom, and the sum of total kinetic energies of two H atoms (after Takahashi *et al.*, 1999b).

our MD simulation (Takahashi *et al.*, 1999a). It was found that the ejection process of the product H₂ via the direct ejection mechanism occurred subsequently after the two H atoms' reaction process. In this mechanism, a part of the excess energy derived from the H₂ formation was absorbed by the ice, and then a part of the remaining excess energy was used for the product H₂ to be ejected from the ice surface.

The ejection rate would be evaluated from the lifetime for the H₂ molecule to escape from the dust surface. The lifetimes of ejection were measured for cases (a) and (b). The re-

sults are shown in Table 6 (after Takahashi *et al.*, 1999a). The temperature dependence and the difference between cases (a) and (b) cannot be discussed clearly, because of the small number of trajectories. The average lifetime as a whole is very short, only about 400–500 fs.

3.6 Product energy distribution

The product energy distribution of H₂ molecules formed on icy mantles of dust grains was also studied (Takahashi *et al.*, 1999b). Figure 4 shows an example of MD trajectories in which H₂ was produced on the surface of amorphous water
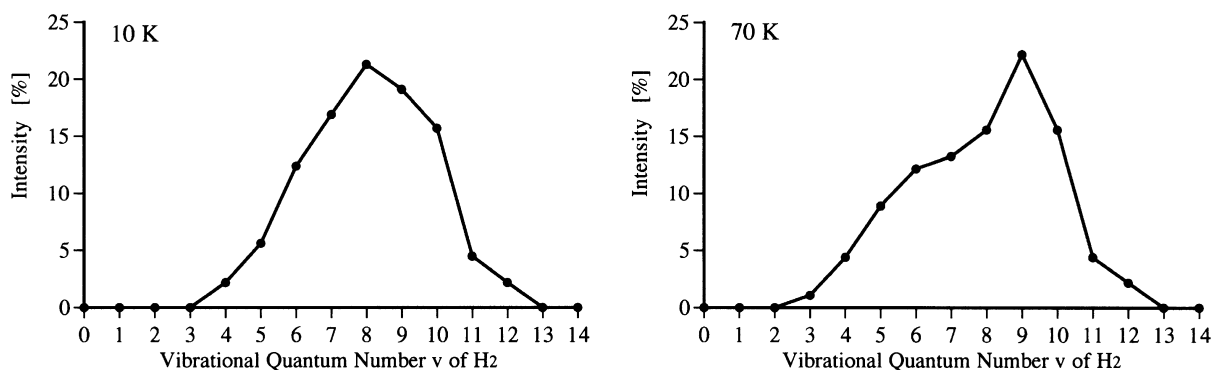
Fig. 5. Vibrational energy population of H_2 formed on the surface of amorphous water ice (after Takahashi *et al.*, 1999b).
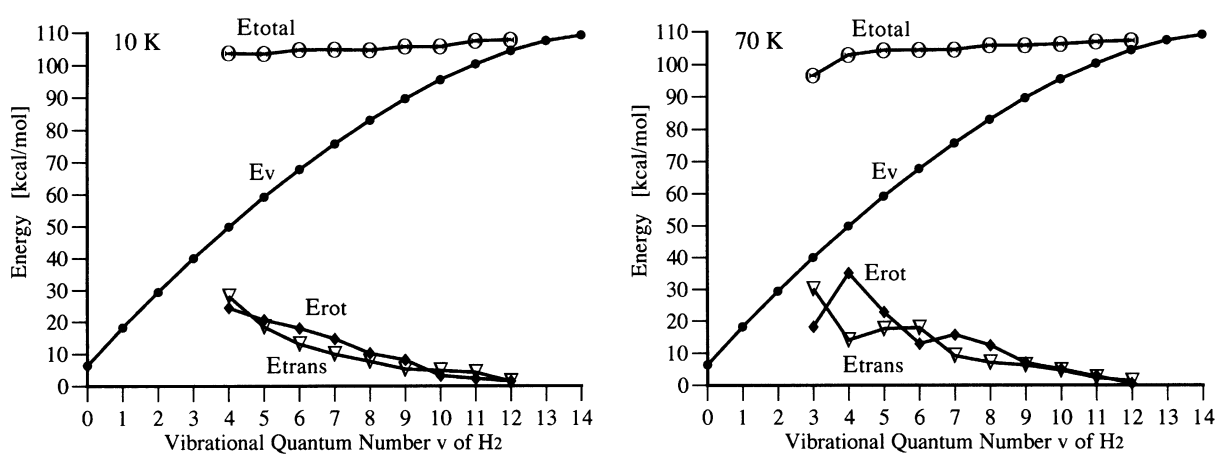

Fig. 6. Total, rotational, and translational energies for each vibrational energy level of H_2.

ice (after Takahashi *et al.*, 1999b). The time dependences of the H–H distance and the height of each H atom are shown in the upper graph. The time origin was taken at the time when the second H atom was thrown onto the surface. The time dependence of the sum of total kinetic energies of two H atoms is shown in the lower graph. The intense oscillation of the H–H distance and the total kinetic energy represents the product H_2 molecule in the vibrationally excited state.

The vibrational energy population for the 10 K and 70 K systems are shown in Fig. 5 (after Takahashi *et al.*, 1999b). It has become clear that H_2 molecules formed on the amorphous water ice are in highly vibrationally excited states. The vibrational energy levels with high populations are around $v = 6$–10. It was found that the vibrational energy population for 70 K is more broadly spread than that for 10 K. It is understood because the surface of the 70 K ice is more random than that of the 10 K ice and that the excess energy released from H_2 formation could be transferred in various ways into the kinetic energies of H_2 on the surface.

The average classical total kinetic, rotational, and translational energies for each vibrational energy level are shown in Fig. 6. It was found that the average total energies are only slightly dependent on the vibrational energy levels. There was found a tendency that the rotational and translational energies decrease as the vibrational energy increases.

The totally averaged vibrational, rotational, translational, and total energies of H_2 formed on the amorphous water ice are shown in Table 7 (after Takahashi *et al.*, 1999b). The results show that the largest part of the H_2 formation energy resides in the vibrational energy of H_2, and the second largest part and the third transfer into rotational and translational energies of H_2, respectively. The average vibrational energy approximately correspond to that for $v = 8$. The evaluated rotational and translational temperatures were, respectively, 5,000–6,000 K and 4,000–5,000 K. It has become clear that the H_2 molecule formed on the amorphous water ice should be in highly excited states not only vibrationally but also rotationally and translationally. The energy absorbed by ice is also shown in Table 7, which was evaluated from the difference between the total energy of the ejected H_2 and the H_2 formation energy, 109.5 kcal/mol. It was found that only a small part of H_2 formation energy was absorbed by the amorphous water ice.

In the present model where H_2O molecules are treated rigid, it is considered that the vibrational energy population is spread over the region of the more highly excited states than in another model where intramolecular modes of H_2O molecules are taken into account. When H_2O molecules have only intermolecular modes, the transfer of the H_2 formation energy into the rotational and translational energies

Table 7. Average product energy distribution of H_2 formed on 10 K and 70 K ice. The numbers in parentheses are the percentages divided by the H_2 formation energy, 109.5 kcal/mol (after Takahashi *et al.*, 1999b).

Temperature		Average product energies of H_2 formed on ice				Energy absorbed
Ice	H atom	E_{vib}	E_{rot}	E_{trans}	E_{total}	by ice
[K]	[K]	[kcal/mol] (%)	[kcal/mol] (%)	[kcal/mol] (%)	[kcal/mol] (%)	[kcal/mol] (%)
10	10	86.0 (78.5)	10.9 (9.9)	8.1 (7.4)	105.1 (96.0)	4.4 (4.0)
70	70	84.0 (76.7)	11.9 (10.7)	9.3 (8.5)	105.2 (96.1)	4.3 (3.9)

of H_2 will become less easy, and the H_2 formation energy is more likely to reside in the vibrational energy of H_2. On the other hand, when H_2O molecules have both intermolecular and intramolecular modes, the H_2 formation energy can be transferred into rotational and translational energies of H_2 more easily (Takahashi *et al.*, 1999b).

As a result of classical MD simulation, the vibrational energy of H_2 obtained here might be overestimated while rotational and translational energies underestimated. If the system is treated quantum mechanically, the extra energy corresponding to the difference between the classical vibrational energy and the nearest lower quantum vibrational energy level would be transferred into rotational and translational energies. The evaluated maximum error is considered to be the extent of energy between one vibrational energy level and the adjacent one. On the other hand, it is considered that the vibrational energy population shown in Fig. 5 is realistic, since we regarded classical vibrational energy between the energy levels v and $v + 1$ as being at the level v.

4. Conclusions

The aim of the present work exists in studying the whole formation process of H_2 on the surface of icy mantles of interstellar dust grains and the resulting product energy distribution of H_2 by using a single model. We performed classical molecular dynamics (MD) computer simulation, where the amorphous water ice slab was generated under periodic boundary conditions as a model surface for icy mantles of dust grains and then the first and the second incident H atoms were thrown onto the surface. In this simulation, the dynamics of all of the atoms and molecules in the system was considered, and thus the energy transfer from H atoms and H_2 to the amorphous ice surface was explicitly taken into account.

The amorphous water ice slabs generated by our MD simulation were compared with those produced experimentally, and we conclude that they are good models for the surface of icy mantles of dust grains. The following fundamental processes of H_2 formation on the icy surface of dust grains were investigated in detail; 1) sticking of incident H atoms onto the dust surface, 2) diffusion of H atoms over the surface, 3) reaction of two H atoms on the surface, and 4) ejection of product H_2 molecule from the surface back into the gas phase. The sticking probability, the mobility before and after H atom is trapped on the surface, reaction probability, and ejection lifetime were obtained for the above processes.

The product energy analysis of H_2 formed on the surface of icy mantles of dust grains was performed based on results of the present MD simulation. It has become clear that the H_2 molecules formed on the icy surface are in highly vibrationally excited states. It was also found that they are in

highly excited states rotationally and translationally. Since the present model is based on a classical MD simulation and a rigid H_2O approximation, the vibrational energy of H_2 obtained here might be slightly overestimated. The influence on the Langmuir-Hinshelwood reaction case by a thermal hopping or tunneling of H atoms after they are once trapped on the ice surface are also neglected here. In spite of these limitation, it is considered that this result reveals the importance of the formation pumping mechanism in the detection of highly excited H_2 molecules. It might be suggested that the rovibrational emission would be detectable even in dark clouds or in regions without a source of UV pumping or collisional excitation (Duley and Williams, 1986, 1993).

References

Buch, V., Identification of two distinct structual and dynamical domains in an amorphous water cluster, *J. Chem. Phys.*, **93**, 2631–2639, 1990.

Buch, V. and J. P. Devlin, Preferential adsorption of ortho-H_2 with respect to para-H_2 on the amorphous ice surface, *J. Chem. Phys.*, **98**, 4195–4206, 1993.

Buch, V. and J. P. Devlin, Interpretation of the 4141 inverse centimeters (2.415 microns) interstellar infrared absorption feature, *Astrophys. J.*, **431**, L135–L138, 1994.

Buch, V. and Q. Zhang, Sticking probability of H and D atoms on amorphous ice: computational study, *Astrophys. J.*, **379**, 647–652, 1991.

Duley, W. W. and D. A. Williams, The formation of interstellar H_2 on amorphous silicate grains, *Mon. Not. R. Astron. Soc.*, **223**, 177–182, 1986.

Duley, W. W. and D. A. Williams, The formation of H_2 on interstellar dust, *Mon. Not. R. Astron. Soc.*, **260**, 37–42, 1993.

Fletcher, N. H., *The Chemical Physics of Ice*, 264 pp., Cambridge University Press, London, 1970.

Flubacher, P., A. J. Leadbetter, and J. A. Morrison, Heat capacity of ice at low temperatures, *J. Chem. Phys.*, **33**, 1751–1755, 1960.

Hansen, J. P. and I. R. McDonald, *Theory of Simple Liquids* (2nd edition), 547 pp., Academic Press, New York, 1986.

Herbst, E., Chemistry in the interstellar medium, *Annu. Rev. Phys. Chem.*, **46**, 27–53, 1995.

Herzberg, G., *Molecular Spectra and Molecular Structure I. Spectra of Diatomic Molecules* (2nd edition), 620 pp., Van Nostrand, New York, 1950.

Hollenbach, D. and E. E. Salpeter, Surface adsorption of light gas atoms, *J. Chem. Phys.*, **53**, 79–86, 1970.

Hunter, D. A. and W. D. Watson, The translational and rotational energy of hydrogen molecules after recombination on interstellar grains, *Astrophys. J.*, **226**, 477–482, 1978.

Jenniskens, P. and D. F. Blake, Structual transitions in amorphous water ice and astrophysical implications, *Science*, **265**, 753–756, 1994.

Jenniskens, P., D. F. Blake, M. A. Wilson, and A. Pohorille, High-density amorphous ice, the frost on interstellar grains, *Astrophys. J.*, **455**, 389–401, 1995.

Jorgensen, W. L., The revised TIPS for simulations of liquid water and aqueous solutions, *J. Chem. Phys.*, **77**, 4156–4163, 1982.

Leitch-Devlin, M. A. and D. A. Williams, Sticking coefficients for atoms and molecules at the surfaces of interstellar dust grains, *Mon. Not. R. Astron. Soc.*, **213**, 295–306, 1985.

Masuda, K. and J. Takahashi, The sticking probability of a hydrogen atom onicy mantle, *Adv. Space Res.*, **19**, 1019–1022, 1997.

Masuda, K., J. Takahashi, and T. Mukai, Sticking probability and mobility of a hydrogen atom on icy mantle of dust grains, *Astron. Astrophys.*, **330**, 773–781, 1998.

Takahashi, J., M. Nagaoka, and K. Masuda, Quantum mechanical treatment for the diffusion process of a hydrogen atom on the amorphous water ice surface, *Int. J. Quantum Chem.*, **70**, 379–385, 1998.

Takahashi, J., K. Masuda, and M. Nagaoka, The formation mechanism of molecular hydrogen on icy mantles of interstellar dust, *Mon. Not. R. Astron. Soc.*, **306**, 22–30, 1999a.

Takahashi, J., K. Masuda, and M. Nagaoka, Product energy distribution of molecular hydrogen formed on icy mantles of interstellar dust, *Astrophys. J.*, **520**, 724–731, 1999b.

Usuda, T., Ph.D. Thesis, Univ. Tokyo, Japan, 1996.

Williams, D. A., Physical and chemical processes on dust, in *Dust and Chemistry in Astronomy*, edited by T. J. Millar and D. A. Williams, Institute of Physics Publishing, Philadelphia, pp. 143–170, 1993.

Zhang, Q. and V. Buch, Computational study of formation dynamics and structure of amorphous ice condensates, *J. Chem. Phys.*, **92**, 5004–5016, 1990.

Zhang, Q., N. Sabelli, and V. Buch, Potential energy surface of H—H$_2$O, *J. Chem. Phys.*, **95**, 1080–1085, 1991.

J. Takahashi (e-mail: junko.takahashi@nao.ac.jp)